Effect of Finite-time DS Controllers on Disturbance Rejection for Planar Bipeds

Daniel S. William and Anne E. Martin

***Abstract*— For many planar bipedal models, each step is divided into a finite time single support period and an instantaneous double support period. During single support, the biped is typically underactuated and thus has limited ability to reject disturbances. The instantaneous nature of the double support period prevents control during this period. However, if the double support period is expanded to finite time, this introduces an overactuated period into the model which may improve disturbance rejection capabilities. This paper derives and compares the performance of two finite-time double support controllers. The first controller uses time to drive the progression of the double support period and controls the joint angles. The second controller uses a time-invariant phase variable to drive the progression of the double support period and controls the joint velocities since it is not possible to control the joint positions. The disturbance rejection capabilities of both controllers are then quantified using simulations. The instantaneous double support model is also simulated for comparison. The instantaneous double support model can recover from the largest disturbances but it requires the greatest number of steps to do. The time-based double support controller can recover from the smallest range of disturbances but requires the fewest number of steps for a given perturbation size.**

I. Introduction

A challenge for bipedal gait is preventing falls after a disturbance. For bipedal robots, controllers generally have a low fall risk or are relatively efficient, but not both [1], [2]. For humans, understanding the aspects of gait that affect fall risk could improve quality of life for elderly adults by reducing injuries due to falls [3].

The efficient but less robust planar biped models typically divide the step into a finite-time single support (SS) period and an instantaneous double support (DS) period (e.g. [4]–[6]). Because the DS period is instantaneous, it is also uncontrolled. These models typically have N rigid links connected by $N-1$ revolute joints with actuators at each joint. They typically have point [4] or curved [5] feet, so the foot cannot apply a moment to the ground. The model has N degrees of freedom (DOF) during SS, and $N-2$ DOF during DS due to the additional foot contact. As a result, the SS period is underactuated while the DS period would be overactuated. During SS, these bipeds cannot directly control their global orientation, which limits their ability to reject disturbances. Steps are typically parameterized using a phase variable, which measures step progression as a function of global orientation. These models are typically controlled using hybrid zero dynamics (HZD) [4], [6]. Under HZD control, a nominal output function parameterized by a phase variable is tracked using input-output linearization. If the biped is perturbed forward (or backward), the phase variable increases (or decreases) and speeds up (or slows down) the rest of the gait cycle while keeping the coordination between joints consistent with an unperturbed step [7].

Because both feet must be on the ground during DS, keeping the joint coordination consistent is equivalent to ensuring that the total configuration of the biped is consistent at the start of every DS period. In contrast, it does not ensure that the velocity of the biped is consistent. Incorrect velocity often causes falls. One method to correct velocity disturbances is to adjust the SS controller based on error in the unactuated velocity [8]. An alternative approach is to take advantage of the overactuation during a finite-time DS. Overactuation is useful because it provides an infinite number of ways to accomplish the same task, so a secondary goal can also be achieved. As a result, the biped can both generate a desired motion and reject disturbances during DS. While there has been limited work comparing the disturbance rejection capabilities of bipeds with uncontrolled vs. controlled DS periods, it does appear that a controlled DS period may be advantageous. For very simple models with variability, a flat-foot model with finite-time DS periods [9] was able to walk with much higher levels of variability than a passive point-foot model [10]. Further, it appears that lengthening the DS period in human gait (typically by walking more slowly) may improve stability [11]. Recent work has also shown that humans struggle to voluntarily lengthen DS duration when forced to maintain a constant walking speed, suggesting that they use the longest possible DS duration for a given speed [12]. This may suggest that a long DS duration increases stability.

Given that a controlled, finite-time DS period may increase disturbance rejection, this motivates developing such a controller. Several controllers have been proposed but the disturbance rejections capabilities of each have yet to be quantified. Existing DS controllers can be broadly divided into time-based and phase-based controllers. For the time-based controllers, the desired motion during DS is parameterized as a function of time (e.g. [13]–[17]). In most cases, the desired motion is specified using joint angles. The required joint torques can be partially determined using input-output linearization [13]. Because the system is overactuated, additional

This work was supported by the NSF under award 1727540. The authors are with the Department of Mechanical and Nuclear Engineering, The Pennsylvania State University, University Park, PA.

conditions such as tracking a ground reaction force (GRF) must be specified to uniquely define the joint torques. However, it may be unnecessary to directly control the GRF as long as the resulting GRF keep the feet firmly planted on the ground. Thus, another option is to use the overatuation to minimize the norm of the joint torques to reduce energy expenditure. The main disadvantage of a time-based controller for an HZD-based model is that it switches between a time-invariant and a time-variant control paradigm between step periods.

Phase-based DS controllers are less studied. The simplest option is to simply ignore the overactuation and not control the position of one DOF so that the biped behaves as if it were underactuated even during the DS period [18], [19]. This allows the same control method to be used for both SS and DS. While this is appealing from a consistency standpoint, it does not take advantage of the overactuation. A more sophisticated version controls both $N-3$ joint positions plus the velocity of the phase variable [20]. This approach uses the same theoretical framework for both gait periods and utilizes the overactuation in the DS period. However, we opted to investigate the novel approach of controlling the velocity of the DS period rather than the position. This may work well because the SS controller handles position control well but not velocity control. By controlling the velocity during DS, the biped ends DS at (or closer to) the desired velocity.

To evaluate the effect of the DS controller on disturbance rejection, three DS controllers are derived and tested in simulation. The first "controller" is simply an instantaneous and unactuated DS period as is common for HZD-based bipeds. The second controller is a time-based position controller that specifies the desired configuration throughout the DS period as a function of time. The third controller is a phase-based velocity controller that specifies the desired velocity throughout the DS period as a function of a phase variable. In contrast to much of the previous work on finite-time DS controllers, we chose to deal with the overactuation by minimizing the norm of the joint torques rather than controlling one of the GRF. Minimizing only the joint torques is not trivial because they are derived as a function of the GRF, which are dependent on the joint torques. For all three DS scenarios, phase-based HZD control is used for SS. To test the disturbance rejection capabilities, velocity disturbances are applied to each of the three models and the system response is quantified.

II. Model Development

As is typical, the planar biped model consists of N rigid links with $N-1$ revolute joints (Fig. 1) [4], [5]. It has either point or curved feet. Several assumptions are made that simplify the actuation and the description of motion of the biped:

M1. Without loss of generality, angle q_1 is unactuated and measured relative to the inertial frame;
M2. angles $q_2 \dots q_N$ are actuated relative joint angles;
M3. the actuators are ideal and have no losses;
M4. the motion is only in the sagittal plane; and
M5. when in contact with the ground, the feet do not slip or lift up except at the end of the stance phase.

A full step consists of four parts—a SS period, an instantaneous, impulsive transition to DS, a DS period, and an instantaneous, smooth transition to SS. The SS period, when only one foot is in contact with the ground, is always finite time. The DS period, when both feet are in contact with the ground, is either instantaneous or finite time. When the DS period is instantaneous, the transitions into and out of DS occur at the same instant as the DS period itself. The SS period ends and the DS period begins when the swing foot impacts the ground. If the other foot does not immediately lift up, the DS period is finite time. This adds another assumption about the biped motion.

M6. The SS period is followed immediately by a transition to the DS period, and the DS period is followed immediately by a transition to the SS period.

The dynamic motion of the model is described with the equation of motion (EOM)

$$\mathbf{D}(\mathbf{q})\ddot{\mathbf{q}} + \mathbf{C}(\mathbf{q},\dot{\mathbf{q}})\dot{\mathbf{q}} + \mathbf{G}(\mathbf{q}) = \mathbf{B}\mathbf{u} + \mathbf{A}(\mathbf{q})^T\lambda, \tag{1}$$

where $\mathbf{q} = \begin{bmatrix} q_1 & \dots & q_N & x_h & y_h \end{bmatrix}^T$ is the extended generalized coordinates, x_h and y_h are the horizontal and vertical position of the hip, $\mathbf{u} = \begin{bmatrix} u_2 \dots u_N \end{bmatrix}^T$ is the joint torques, and λ is the set of Lagrangian constraint forces corresponding to the GRF. The matrices $\mathbf{D} \in \mathbb{R}^{(N+2)\times(N+2)}$ is the inertia matrix, $\mathbf{C} \in \mathbb{R}^{(N+2)\times(N+2)}$ contains the Coriolis and centripetal force terms, $\mathbf{G} \in \mathbb{R}^{(N+2)\times 1}$ is the gravity vector, $\mathbf{B} \in \mathbb{R}^{(N+2)\times(N-1)}$ maps the control inputs to joint torques, and $\mathbf{A}$ is the Jacobian constraint matrix. During SS, the biped only has one foot on the ground, so there is one GRF with two components, $\lambda \in \mathbb{R}^2$. During DS, the biped has both feet on the ground, so there are two GRF with a total of four components, $\lambda \in \mathbb{R}^4$. During SS, $\mathbf{A} \in \mathbb{R}^{(N+2)\times 2}$ is found via $\mathbf{A} = \frac{\partial \mathbf{p}}{\partial \mathbf{q}}$, where $\mathbf{p}$ is the position of the stance foot with respect to the hip, accounting for any curved foot roll [5]. During DS, $\mathbf{A} \in \mathbb{R}^{(N+2)\times 4}$ is found via $\mathbf{A} = \begin{bmatrix} \mathbf{A}_\ell & \mathbf{A}_t \end{bmatrix}^T$, where $\mathbf{A}_\ell = \frac{\partial \mathbf{p}_\ell}{\partial \mathbf{q}}$, $\mathbf{A}_t = \frac{\partial \mathbf{p}_t}{\partial \mathbf{q}}$, $\mathbf{p}_\ell$ is the position of the leading foot, and $\mathbf{p}_t$ is the position of the trailing foot, both with respect to the hip and accounting for any curved foot roll.

Eq. 1 can also be written

$$\ddot{\mathbf{q}} = \mathbf{D}^{-1}\left(\mathbf{A}^T\lambda - \mathbf{C}\dot{\mathbf{q}} - \mathbf{G}\right) + \mathbf{D}^{-1}\mathbf{B}\mathbf{u}, \tag{2}$$

or as a first order system

$$\begin{aligned} \dot{\mathbf{x}} &= \begin{bmatrix} \dot{\mathbf{q}} \\ \mathbf{D}^{-1}\left(\mathbf{A}^T\lambda - \mathbf{C}\dot{\mathbf{q}} - \mathbf{G}\right) \end{bmatrix} + \begin{bmatrix} \mathbf{0} \\ \mathbf{D}^{-1}\mathbf{B} \end{bmatrix} \cdot \mathbf{u} \\ &= \mathbf{f}(\mathbf{x},\lambda) + \mathbf{g}(\mathbf{x}) \cdot \mathbf{u}, \end{aligned} \tag{3}$$

where $\mathbf{x} = \begin{bmatrix} \mathbf{q}^T & \dot{\mathbf{q}}^T \end{bmatrix}^T$.

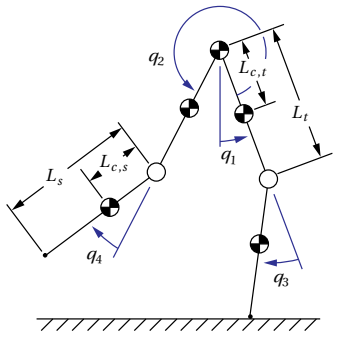

Fig. 1. A diagram of the four link biped model. The unactuated angle is q_1 and the actuated angles are q_2, q_3, and q_4.

The constraint equation $\mathbf{A}\dot{\mathbf{q}} = \mathbf{0}$ ensures that the biped is correctly attached to the ground in the extended coordinate system. The validity of this constraint is verified later by checking that the vertical ground reaction force is positive and that the horizontal ground reaction force is within the cone of friction. If the constraint forces violate these assumptions, the step has failed. To use the constraint equation with the EOM, it is differentiated once

$$\mathbf{A}\ddot{\mathbf{q}} = -\dot{\mathbf{A}}\dot{\mathbf{q}}. \tag{4}$$

When the constraint equation (4) is combined with the EOM (2), the system has N DOF during SS and $N-2$ DOF during DS. Because the number of actuators $(N-1)$ remains constant, the biped is underactuated during SS and overactuated during DS.

Both a SS and DS controller are required to actuate a single step. Three different DS scenarios will be compared, an instantaneous impact with no controller, a time-based finite-time controller, and a phase-based finite-time controller. The following sections will derive each controller and outline the differences between them.

A. Single Support

For all DS scenarios, the same SS controller is used. This controller uses input-output linearization and is identical to the controller given by [4], [5]. A brief derivation is included for completeness and to aid in comparisons with DS controllers. The desired angles are parameterized as a function of a phase variable, θ [4]:

$$\theta(\mathbf{q}) = \mathbf{c}\mathbf{q}, \tag{5}$$

where $\mathbf{c} \in \mathbb{R}^{1\times N+2}$. For this work, θ is the linearized progression of the hip. θ is then normalized to lie between 0 and 1 for a nominal step.

$$s = \frac{(\theta(\mathbf{q}) - \theta^+)}{(\theta^- - \theta^+)}, \tag{6}$$

where θ^+ and θ^- are the values of θ at the beginning and end of the nominal step, respectively.

The following assumptions must hold during the SS period to ensure that the gait is valid:

S1. The swing leg begins behind the hip and ends in front of the hip;
S2. the SS phase ends when the swing foot makes contact with the ground; and
S3. the phase variable is strictly monotonic and uncontrolled.

The control input of the system is solved via input-output linearization [21]. The output function describes the desired position of the actuated joints. This output function will be zero when the motion of the biped follows the desired trajectories, leading to the following error equation for the system's output.

$$\mathbf{y} = \mathbf{h}(\mathbf{q}) = \mathbf{H_0}\mathbf{q} - \mathbf{h_d}(s(\mathbf{q})), \tag{7}$$

where $\mathbf{H_0} \in \mathbb{R}^{N-1\times N+2}$ maps the generalized coordinates to the controlled DOF and $\mathbf{h_d}$ is the desired joint trajectories, given as a function of step progression. To drive the output to zero, the output function is differentiated twice, and the EOM (2) is substituted into the equation, resulting in

$$\ddot{\mathbf{y}} = \mathscr{L}_f^2\mathbf{h} + \mathscr{L}_g\mathscr{L}_f\mathbf{h}\cdot\mathbf{u}, \tag{8}$$

where $\mathscr{L}_f^2\mathbf{h} \triangleq \frac{\partial}{\partial \mathbf{x}}\left(\frac{\partial \mathbf{h}}{\partial \mathbf{x}}\mathbf{f}\right)\mathbf{f}$ and $\mathscr{L}_g\mathscr{L}_f\mathbf{h} \triangleq \frac{\partial}{\partial \mathbf{x}}\left(\frac{\partial \mathbf{h}}{\partial \mathbf{x}}\mathbf{f}\right)\mathbf{g}$ are Lie derivatives [21]. To zero any errors, set $\ddot{\mathbf{y}} = \mathbf{v}$, where $\mathbf{v}$ is a stabilizing controller such as $\mathbf{v} = k_p\mathbf{y} + k_v\dot{\mathbf{y}}$ (a PD controller) and solve for $\mathbf{u}$. This gives

$$\begin{aligned}\mathbf{u} &= \mathscr{L}_g\mathscr{L}_f\mathbf{h}^{-1}(\mathbf{v} - \mathscr{L}_f^2\mathbf{h}) \\ &= \left(\tfrac{\partial \mathbf{h}}{\partial \mathbf{q}}\mathbf{D}^{-1}\mathbf{B}\right)^{-1}\left(\mathbf{v} - \tfrac{\partial^2 \mathbf{h_d}}{\partial \theta^2}(\mathbf{c}\dot{\mathbf{q}})^2 - \tfrac{\partial \mathbf{h}}{\partial \mathbf{q}}\mathbf{D}^{-1}\left(\mathbf{A}^T\lambda - \mathbf{G} - \mathbf{C}\dot{\mathbf{q}}\right)\right).\end{aligned} \tag{9}$$

Because $\mathbf{u} = \mathbf{u}(\mathbf{q}, \dot{\mathbf{q}}, \lambda)$, (2), (4), and (9) need to be solved concurrently to find the acceleration $\ddot{\mathbf{q}}$, input $\mathbf{u}$, and Lagrangian constraints λ.

B. Instantaneous Impact

The transition to DS always begins when the swing foot impacts the ground. This section derives the impact mapping, which is essentially equivalent to the models given by [4], [5]. For the time- and phase-based controllers, the impact is followed by a finite-time DS period. For the scenario with no DS controller, the swing foot just before impact becomes the new stance foot and the stance foot just before impact immediately lifts and becomes the new swing foot. The impact must satisfy the following assumptions:

I1. The transition to the DS period occurs instantaneously via an impact of the swing foot;
I2. the stance foot does not slip or lift up after impact;
I3. joint torques do not apply impulsive actuation; and
I4. the biped position does not change during impact.

During the instantaneous impact, the heelstrike of the swing foot causes the velocity of the hip to change direction. The EOM of the impact event is still given by (1). To determine the change in velocities and the GRF, (1) is integrated over the duration of the impact. This is then simplified using the assumptions to give

$$\mathbf{D}(\mathbf{q})\dot{\mathbf{q}}^+ - \mathbf{D}(\mathbf{q})\dot{\mathbf{q}}^- = \mathbf{A}^T\mathbf{f}_\lambda, \tag{10}$$

where $\mathbf{f}_\lambda$ are the integrated impulsive GRF, and $\dot{\mathbf{q}}^-$ and $\dot{\mathbf{q}}^+$ are the joint velocities just before and just after impact, respectively. The assumption of no slip or rebound leads to the following constraint equation

$$\mathbf{A}\dot{\mathbf{q}}^+ = \mathbf{0}, \tag{11}$$

where $\mathbf{A}$ is given in Section II. For the instantaneous DS case, $\mathbf{A}$ is used from the SS model, and for a finite-time DS, $\mathbf{A}$ is taken from the DS model. The velocity after impact $\dot{\mathbf{q}}^+$ and the impulse on the foot (or feet) $\mathbf{f}_\lambda$ can be found by solving (10) and (11). At the end of the impact, the coordinates are relabeled so that the leading leg is the stance leg and the trailing leg is the swing leg.

C. Double Support - Time

For the next two scenarios, the DS period is finite time. The derivation of these controllers differs from the SS controller due to the overactuation. As a result, the output function can only define the trajectory of $N-2$ coordinates independently. The remaining 2 coordinates are defined by assumption M5. Given that there are $N-1$ actuators, the equations must be manipulated to minimize the norm of $\mathbf{u}$. This section will derive the time-based DS controller.

Instead of the time-invariant phase variable used in the SS controller, the time-based DS controller simply uses normalized time to measure the progression of the biped through DS.

$$s = \frac{(t - t_f)}{(t_f)}, \tag{12}$$

where t is the current time and t_f is the planned duration of the DS period, defined a priori. The time t is always set to 0 at the beginning of DS.

The controller is found via input-output linearization. The output function defines the desired motion of $N-2$ joint angles. The process to determine the control input is analogous to that of the SS control model, but the output function is different.

$$\mathbf{y} = \mathbf{h}(\mathbf{q}, t) = \mathbf{H_{0,DS}}\mathbf{q} - \mathbf{h_d}(s(t)), \tag{13}$$

where $\mathbf{H_{0,DS}} \in \mathbb{R}^{(N-2)\times(N+2)}$ is the mapping between the extended coordinate system and the controlled joint trajectories. The output (13) is differentiated twice, the EOM (2) is substituted into the equation, and the acceleration of the output is replaced with the feedback controller. The result has the same form as (9), but because the output (13) is different, the final result becomes

$$\mathbf{u} = \left(\mathbf{H_{0,DS}}\mathbf{D}^{-1}\mathbf{B}\right)^{-1}\left(\mathbf{v} + \mathbf{H_{0,DS}}\mathbf{D}^{-1}\left(\mathbf{C}\dot{\mathbf{q}} + \mathbf{G} - \mathbf{A}^T\lambda\right) - \frac{\mathrm{d}^2\mathbf{h_d}}{\mathrm{d}t^2}\right), \tag{14}$$

where $\mathbf{v} = k_p\mathbf{y} + k_d\dot{\mathbf{y}}$ is the PD controller and $\left(\mathbf{H_{0,DS}}\mathbf{D}^{-1}\mathbf{B}\right) \in \mathbb{R}^{(N-2)\times(N-1)}$. While (14) gives an equation for $\mathbf{u}$, it cannot be used directly because λ is unknown. Finding the solution would be straightforward if we wanted to minimize the norm of all of the unknowns. However, we wish to minimize only the norm of $\mathbf{u}$, so an equation for $\mathbf{u}$ without any unknowns must be found. To do so, we substitute (2) into (4) and solve for λ

$$\lambda = \underbrace{\left(\mathbf{A}\mathbf{D}^{-1}\mathbf{A}^T\right)^{-1}\left(\mathbf{A}\mathbf{D}^{-1}(\mathbf{C}\dot{\mathbf{q}} + \mathbf{G}) - \dot{\mathbf{A}}\dot{\mathbf{q}}\right)}_{\lambda_1(\mathbf{q},\dot{\mathbf{q}})} - \underbrace{\left(\mathbf{A}\mathbf{D}^{-1}\mathbf{A}^T\right)^{-1}\mathbf{A}\mathbf{D}^{-1}\mathbf{B}}_{\lambda_2(\mathbf{q})}\cdot\mathbf{u}. \tag{15}$$

This is then substituted into (2) to give

$$\begin{aligned}\ddot{\mathbf{q}} &= \mathbf{f}^*(\mathbf{q}, \dot{\mathbf{q}}) + \mathbf{g}^*(\mathbf{q})\mathbf{u} \\ &= \mathbf{D}^{-1}\left(\mathbf{A}^T\lambda_1 - \mathbf{C}\dot{\mathbf{q}} - \mathbf{G}\right) + \mathbf{D}^{-1}\left(\mathbf{B} + \mathbf{A}^T\lambda_2\right)\mathbf{u}.\end{aligned} \tag{16}$$

Finally, (16) can be used in the input-output linearization to calculate an alternate form of (14).

$$\mathbf{u} = \left(\mathbf{H_{0,DS}}\mathbf{g}^*\right)^{-1}\left(\mathbf{v} + \frac{\mathrm{d}^2\mathbf{h_d}}{\mathrm{d}t^2} - \mathbf{H_{0,T}}\mathbf{f}^*\right), \tag{17}$$

where $\left(\mathbf{H_{0,DS}}\mathbf{g}^*\right) \in \mathbb{R}^{(N-2)\times(N-1)}$, so a pseudoinverse is used to solve for $\mathbf{u}$. To find the remaining unknowns, $\mathbf{u}$ is then substituted back into (15) and (16).

D. Double Support - Phase

The final scenario uses a phase-based DS controller. In contrast to the other controllers, this controller specifies joint velocities instead of joint angles. As described later, it is not possible to directly control the joint angles with this formulation, even if desired.

Because this is a phase-based controller, a phase variable is used to measure the step progression. Due to the overactuation during DS, the phase variable is different than the one used during SS. During SS, one of the DOF is unactuated and the progression of this unactuated DOF serves as a measure of step progression. The phase variable must be uncontrolled; otherwise the phase variable does not evolve independent of the control effort. During DS, all of the system's DOF are directly controllable, so the phase variable was chosen to be the momentum conjugate to the absolute angle [20].

$$\theta(\mathbf{q}, \dot{\mathbf{q}}) = \mathbf{D_1}(\mathbf{q})\dot{\mathbf{q}}, \tag{18}$$

where $\mathbf{D}_1(\mathbf{q})$ is the first row of the inertia matrix. This can be thought of as the whole body momentum and was chosen because it is monotonic, uncontrollable, and a measure of the biped state in an inertial frame. The step progression s is normalized as in (6).

The phase-based DS controller is found via input-output linearization. Unlike the other controllers, the output function defines the desired velocity of $N-2$ joints,

$$\mathbf{y} = \mathbf{h}(\mathbf{q}, \dot{\mathbf{q}}) = \mathbf{H_{0,DS}}\dot{\mathbf{q}} - \mathbf{h_d}(s(\mathbf{q}, \dot{\mathbf{q}})). \tag{19}$$

To calculate $\mathbf{u}$, the output (19) is differentiated, the EOM (2) is substituted into the equation, and the acceleration of the output is replaced with a feedback controller.

$$\begin{aligned}\mathbf{u} &= \mathscr{L}_g\mathbf{h}^{-1}\left(\mathbf{v} - \mathscr{L}_f\mathbf{h}\right) \\ &= \left(\left(\mathbf{H_{0,DS}} + \frac{\partial\mathbf{h_d}}{\partial\theta}\frac{\partial\theta}{\partial\dot{\mathbf{q}}}\right)\mathbf{D}^{-1}\mathbf{B}\right)^{-1}\left(\mathbf{v} + \frac{\partial\mathbf{h_d}}{\partial\theta}\frac{\partial\theta}{\partial\mathbf{q}}\dot{\mathbf{q}} - \right. \\ &\qquad \left.\left(\mathbf{H_{0,DS}} - \frac{\partial\mathbf{h_d}}{\partial\theta}\frac{\partial\theta}{\partial\dot{\mathbf{q}}}\right)\left(\mathbf{A}^T\lambda - \mathbf{C}\dot{\mathbf{q}} - \mathbf{G}\right)\right),\end{aligned} \tag{20}$$

where $\mathbf{v} = k_p\mathbf{y}$ is the proportional controller, $\mathscr{L}_f\mathbf{h} \triangleq \frac{\partial \mathbf{h}}{\partial \mathbf{x}}\mathbf{f}$ and $\mathscr{L}_g\mathbf{h} \triangleq \frac{\partial \mathbf{h}}{\partial \mathbf{x}}\mathbf{g}$. $\mathscr{L}_g\mathbf{h} \in \mathbb{R}^{(N-2)\times(N-1)}$ matrix is inverted using a pseudoinverse. Because the output is a function of $\dot{\mathbf{q}}$, and thus relative degree one, it is only differentiated once.

If the output function defined the desired joint angles, then the inverted matrix $\mathscr{L}_g\mathbf{h}$ would be singular, because $\mathbf{y}$ would be given by $\mathbf{H_{0,DS}q} - \mathbf{h_d}(s(\mathbf{q},\dot{\mathbf{q}}))$ and $\mathscr{L}_g\mathbf{h} = \frac{\partial \mathbf{h_d}}{\partial \theta}\frac{\partial \theta}{\partial \dot{\mathbf{q}}}\mathbf{g}$. To see why this is a singular matrix, we will consider the rank of the first two terms. $\frac{\partial \mathbf{h_d}}{\partial \theta} \in \mathbb{R}^{(N-2)\times 1}$ is rank 1 and $\frac{\partial \theta}{\partial \dot{\mathbf{q}}} \in \mathbb{R}^{1\times(N+2)}$ is rank 1. Therefore, the resulting product is at most rank 1 [22]. Because $1 < (N-2)$ it is not possible to invert this matrix, even using the pseudoinverse. On the other hand, because $\mathbf{y}$ is defined as in (17), $\mathscr{L}_g\mathbf{h} = \left(\mathbf{H_{0,DS}} + \frac{\partial \mathbf{h_d}}{\partial \theta}\frac{\partial \theta}{\partial \dot{\mathbf{q}}}\right)\mathbf{g}$. While $\frac{\partial \mathbf{h_d}}{\partial \theta}\frac{\partial \theta}{\partial \dot{\mathbf{q}}}$ is still rank 1, it is added to $\mathbf{H_{0,DS}}$ with rank $N-2$. So the resulting sum and its product with $\mathbf{g}$ has rank $N-2$. Therefore, this can be inverted using a pseudoinverse.

As with the time-based DS controller, (2), (4), and (20) are manipulated to minimize the norm of $\mathbf{u}$ without minimizing $\ddot{\mathbf{q}}$ or λ. Briefly, we write the EOM as in (16) and substitute it into the input-output feedback linearization equation (20) to obtain

$$\mathbf{u} = \left(\left(\mathbf{H_{0,DS}} + \frac{\partial \mathbf{h_d}}{\partial \theta}\frac{\partial \theta}{\partial \dot{\mathbf{q}}}\right)\mathbf{g}^*\right)^{-1}\left(\mathbf{v} + \frac{\partial \mathbf{h_d}}{\partial \theta}\frac{\partial \theta}{\partial \mathbf{q}} - \left(\mathbf{H_{0,DS}} - \frac{\partial \mathbf{h_d}}{\partial \theta}\frac{\partial \theta}{\partial \dot{\mathbf{q}}}\right)\mathbf{f}^*\right), \tag{21}$$

where $\left(\left(\mathbf{H_{0,DS}} + \frac{\partial \mathbf{h_d}}{\partial \theta}\frac{\partial \theta}{\partial \dot{\mathbf{q}}}\right)\mathbf{g}^*\right) \in \mathbb{R}^{(N-2)\times(N-1)}$, so a pseudoinverse is used to solve for $\mathbf{u}$.

E. Transition to SS

The transition to SS always begins at the end of the DS period. For the instantaneous DS model, this occurs simultaneously with the instantaneous transition into DS. For the finite-time DS models, the transition occurs when the vertical GRF for the trailing leg equals 0. The transition to SS is smooth and instantaneous, and is defined by the mapping

$$\begin{bmatrix}\mathbf{q}^+ & \dot{\mathbf{q}}^+\end{bmatrix}^T = \begin{bmatrix}\mathbf{q}^- & \dot{\mathbf{q}}^-\end{bmatrix}^T, \tag{22}$$

where the superscripts $^+$ and $^-$ indicate the instances just after and before the transition, respectively.

III. Simulations

A. Simulation Generation

For the simulations, the model has four links, point feet, and a point mass at the hip (Fig. 1, Table I). The joint angle or velocity trajectories are parameterized by Bezier polynomials with order 5 for SS and order 3 for DS. For the finite-time DS controllers, the knee joints q_3 and q_4 were directly controlled using (17) or (21). To find the gaits, the Bezier polynomials were found using simulated annealing. This technique searched for a set of polynomial coefficients and initial conditions that minimized the objective function and satisfied all of the constraints. The objective function was an integrated torque-squared based function [5]. To implement the constraints, exponential barrier functions were used [23]. These functions were added to the objective function to penalize constraint violations. The primary constraints were that the GRF meet assumption M5 (no slipping and no flying) and that the gait was periodic (the positions and velocities at the beginning of the step were equal to those at the beginning of the following step). Additional constraints, such as limiting joint angles to normal human motion and limiting walking speed and step length to a set range prevented the optimization from exploiting the objective function.

TABLE I

Parameters. The values are the same for both legs.

Parameter	Value	Description
L_s	0.433	Shank Length (m)
L_t	0.431	Thigh Length (m)
$L_{c,s}$	0.177	Shank COM Distance (m)
$L_{c,t}$	0.185	Thigh COM Distance (m)
M_s	4.07	Shank Mass (kg)
M_t	10.43	Thigh Mass (kg)
M_h	53.81	Hip Mass (kg)
J_s	0.175	Shank Moment of Inertia (kg·m^2)
J_t	0.106	Thigh Moment of Inertia (kg·m^2)
k_p	100	Proportional Control Gain
k_d	10	Derivative Control Gain

Because the structure of a step is fundamentally different for the instantaneous DS model compared to the finite-time DS models, the gaits were chosen to be temporally similar. To help ensure this, the optimal gait for the phase-based model was used as the basis for the other two models. For the time-based DS model, the phase-based DS polynomials were transformed into time-based polynomials by simulating the step using the phase-based DS controller, and then fitting the resulting DS position trajectories in the time domain. For the instantaneous DS model, the gait was transformed by simulating the step using the phase-based DS controller, and then fitting the entire resulting step position trajectories in the phase domain, using the SS phase variable (5). Each of the transformed gaits were then optimized to minimize torque squared and meet the step constraints as before. The step lengths and walking speed constraints were very tight to ensure that those key parameters matched very closely for all three scenarios. The resulting gaits for the finite-time DS scenarios were kinematically similar, but the gait for the instantaneous DS scenario was significantly different than the other two as expected (Fig. 2). Despite the differences in the joint angles, step length and walking speed was very similar for all three scenarios, with step length ranging from 0.224 m to 0.230 m and speed ranging from 0.711 m/s to 0.748 m/s.

To allow improved disturbance rejection capabilities, a correction polynomial was added to the nominal Bezier polynomial during DS [24]. This correction polynomial was defined at the start of each DS period to exactly account for the position and velocity errors at the start

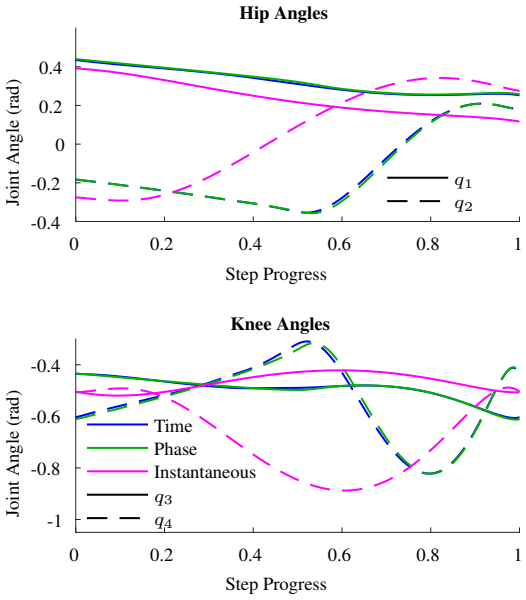

Fig. 2. Joint angles during an unperturbed step from heelstrike to the next heelstrike. The time- and phase-based DS conditions have very similar joint angles, while the instantaneous DS condition has significantly different joint angles. This is due to the differences between the different types of gaits.

of the period and smoothly converge to zero at the end of the nominal period. Because the actual DS period was sometimes shorter than the nominal DS period, errors were not always corrected within one step. Without the correction polynomial, there were often large velocity errors at the start of the DS period that the stabilizing P or PD controller attempted to zero quickly. The more quickly the errors were zeroed, the more likely it was that the feet would slip or lift up. The correction polynomial allowed the errors to be zeroed more evenly across the period and thus increased the disturbance rejection capabilities.

The models were tested to find which controller was more equipped to handle disturbances. Disturbances were created by instantaneously changing the velocities just after the transition to DS, which simulates a horizontal impulsive push on the hip. Two tests were performed. The first test generated a single perturbation for one step, and the number of steps until the gait returned to the nominal gait was recorded. This return was defined as when the horizontal hip velocity at the end of DS was within 0.025% of the nominal value. This value was chosen so that the smallest non-zero perturbation took at least 1 step to recover. Multiple simulations were run, with increasing perturbation magnitude until the biped was unable to recover. Both positive and negative perturbations were tested. The second test introduced a random perturbation every step and the number of steps until the biped fails was recorded. The maximum magnitude of the perturbation increased as the step number increased. 10 different sets of random perturbations were

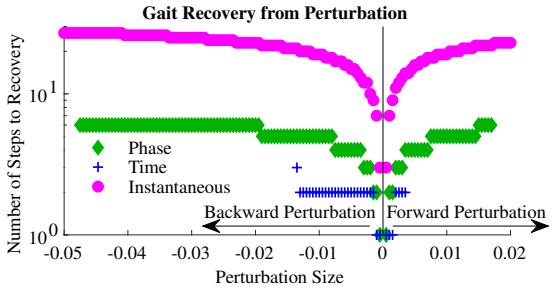

Fig. 3. Ability to recover from perturbations. The horizontal axis indicates the size of the perturbation while the vertical axis indicates the number of steps to return to the nominal periodic gait, plotted on a logarithmic scale. As indicated by the much wider spread of the data, the instantaneous DS model is able to recover from much larger perturbations than either of the finite-time DS controllers. The instantaneous scenario can recover from perturbations larger than indicated here, to at least −0.5 m/s and 0.4 m/s. For the perturbations from which it is able to recover, the time-based controller can recover in the fewest steps.

generated, resulting in 10 trials for each model. The same vector of perturbations was used for all models.

B. Simulation Results

In the single perturbation trials, the phase-based DS model could recover from larger perturbations than the time-based DS model (Fig. 3). The instantaneous impact model could recover from perturbations even larger than the phase-based DS controller model. However, for the perturbations from which the model was able to recover, the time-based controller recovered faster than the phase-based controller, which was able to recover faster than the instantaneous impact model (Figs. 3, 4). This is likely because the instantaneous DS model is unable to control the velocities during the DS instant, and the impulsive impact tends to exaggerate velocity errors. In contrast, the finite-time DS models are able to

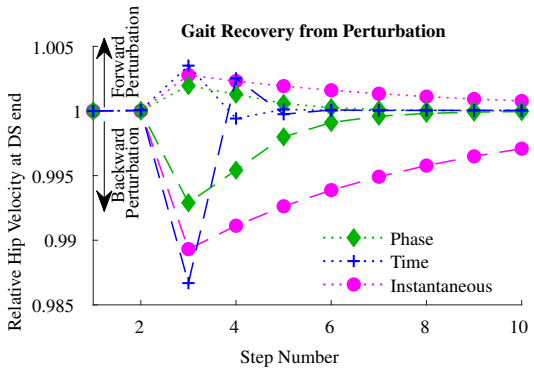

Fig. 4. Typical recovery from a single perturbation. Each controller was perturbed twice, once forward and once backward, and the horizontal hip velocity at the end of DS is shown with markers. The absolute magnitude of the perturbation was the same for all controllers. The phase-based controller requires more steps to recover than the time-based controller and the scenario with an instantaneous DS period takes the largest number of steps to recover.

TABLE II

NUMBER OF STEPS TO FAILURE WITH RANDOM GROWING PERTURBATIONS. 10 TRIALS ARE USED FOR EACH DS CONTROLLERS.

	Instantaneous	Time	Phase
Mean	157.6	7.2	16.3
Max	189	10	26
Min	112	4	10
Standard Deviation	28.8	1.99	4.81

control the velocity of the biped during DS and reduce the velocity error. Despite this, the instantaneous impact model is able to reject much larger perturbations. These results are consistent with the random perturbation trials (Table II). For all 10 random perturbation vectors used, the instantaneous DS controller could walk the longest and the time-based DS controller always failed in the fewest number of steps.

The primary mode of failure for the finite-time DS models was invalid GRF during DS, i.e. the feet would slip or the front foot would lift up. This may be due to the specific four-link biped model used, and a biped with telescopic legs or a kneed biped with six links may be better suited to a finite-time DS period. With a four-link kneed biped, the knees need to travel through a large range of motion to transport the hip through DS and to end with the correct velocity to initiate SS. This requires large horizontal GRF with limited ability to control the direction of the GRF due to the small number of DOF. As a result, it can be difficult to prevent slipping during DS. In contrast, a four-link biped with telescopic legs generates more vertical GRF, so slipping is less likely. A kneed biped with six links has more DOF and can thus better modulate the direction of the GRF to prevent slipping. To address this issue without changing the biped, it may be beneficial to saturate the joint torques. Ideally, this would be done in an adaptive manner such that the maximum joint torque is just below the value that would generate invalid GRF [15]. This is left for future work.

There appears to be an inverse relationship between maximum perturbation size and time to recovery. This is not surprising because faster recovery requires greater GRF to accelerate the biped back to the nominal gait. Larger horizontal GRF also make the biped more likely to slip. Since recovery from large perturbations is likely more important than a quick recovery in most situations, the phase-based DS controller is likely better than the time-based DS controller.

REFERENCES

[1] S. H. Collins, A. Ruina, R. Tedrake, and M. Wisse, "Efficient bipedal robots based on passive-dynamic walkers," *Science*, vol. 307, no. 5712, pp. 1082–85, 2005.

[2] A. Goswami, "Postural stability of biped robots and the foot-rotation indicator (FRI) point," *Int. J. Robot. Res.*, vol. 18, no. 6, pp. 523–533, Jun. 1999.

[3] M. E. Tinetti and C. S. Williams, "The effect of falls and fall injuries on functioning in community-dwelling older persons," *Journal of Gerontology: Medical Sciences*, vol. 53A, no. 2, pp. 112–9, 1998.

[4] E. R. Westervelt, J. W. Grizzle, C. Chevallereau, J. H. Choi, and B. Morris, *Feedback Control of Dynamic Bipedal Robot Locomotion*. CRC Press, 2007.

[5] A. E. Martin and J. P. Schmiedeler, "Predicting human walking gaits with a simple planar model," *J. Biomech.*, vol. 47, no. 6, pp. 1416–21, 2014.

[6] A. E. Martin, D. C. Post, and J. P. Schmiedeler, "Design and experimental implementation of a hybrid zero dynamics-based controller for planar bipeds with curved feet," *Int. J. Robot. Res.*, vol. 33, no. 7, pp. 988–1005, 2014.

[7] D. J. Villarreal, H. A. Poonawala, and R. D. Gregg, "A robust parameterization of human gait patterns across phase-shifting perturbations," *IEEE Trans. Neural Syst. Rehab. Eng.*, vol. 25, no. 3, pp. 265–278, 2017.

[8] D. C. Post and J. P. Schmiedeler, "Velocity disturbance rejection for planar bipeds walking with HZD-based control," in *IROS*, Sept. 2014, pp. 4882–4887.

[9] J. Ahn and N. Hogan, "Long-range correlations in stride intervals may emerge from non-chaotic walking dynamics," *PLoS One*, vol. 8, no. 9, p. e73239, 2013.

[10] M. Garcia, A. Chatterjee, A. Ruina, and M. Coleman, "The simplest walking model: Stability, complexity, and scaling," *J. Biomech. Eng.*, vol. 120, no. 2, pp. 281–8, 1998.

[11] J. B. Dingwell, J. P. Cusumano, P. R. Cavanagh, and D. Sternad, "Local dynamic stability versus kinematic variability of continuous overground and treadmill walking," *J. Biomech. Eng.*, vol. 123, no. 1, pp. 27–32, 2001.

[12] D. S. Williams and A. E. Martin, "Gait modification when decreasing double support percentage," *J. Biomech.*, vol. In review, 2019.

[13] D. Tlalolini, C. Chevallereau, and Y. Aoustin, "Comparison of different gaits with rotation of the feet for a planar biped," *Robot. Auton. Syst.*, vol. 57, no. 4, pp. 371–383, 2009.

[14] R. Dehghani, A. Fattah, and E. Abedi, "Cyclic gait planning and control of a five-link biped robot with four actuators during single support and double support phases," *Multibody Syst. Dyn.*, vol. 33, no. 4, pp. 389–411, 2015.

[15] S. Miossec and Y. Aoustin, "A simplified stability study for a biped walk with underactuated and overactuated phases," *Int. J. Robot. Res.*, vol. 24, no. 7, pp. 537–551, 2005.

[16] F. Zonfrilli, G. Oriolo, and D. Nardi, "A biped locomotion strategy for the quadruped robot Sony ERS-210," in *IROS*, Washington DC, May 2002, pp. 2768–2774.

[17] A. Grishin, A. Formal'sky, A. Lensky, and S. Zhitomirsky, "Dynamic walking of a vehicle with two telescopic legs controlled by two drives," *Int. J. Robot. Res.*, vol. 13, no. 2, pp. 137–147, Apr. 1994.

[18] S. Srinivasan, I. A. Raptis, and E. R. Westervelt, "Low-dimensional sagittal plane model of normal human walking," *J. Biomech. Eng.*, vol. 130, no. 5, p. 051017, 2008.

[19] K. A. Hamed, N. Sadati, W. A. Gruver, and G. A. Dumont, "Stabilization of periodic orbits for planar walking with noninstantaneous double-support phase," *IEEE Trans. Syst. Man Cy. A*, vol. 42, no. 3, pp. 685–706, 2012.

[20] M. Scheint, M. Sobotka, and M. Buss, "Virtual holonomic constraint approach for planar bipedal walking robots extended to double support," in *CDC*, Shanghai, Dec. 2009, pp. 8180–8185.

[21] A. Isidori, *Nonlinear control systems*. Springer Science & Business Media, 2013.

[22] R. B. Bapat, *Linear algebra and linear models*. Springer Science & Business Media, 2012.

[23] G. Rätsch, M. K. Warmuth, S. Mika, T. Onoda, S. Lemm, and K.-R. Müller, "Barrier boosting." in *COLT*, 2000, pp. 170–179.

[24] A. E. Martin and R. D. Gregg, "Incorporating human-like walking variability in an HZD-based bipedal model," *IEEE Trans. Robot.*, vol. 32, no. 4, pp. 943–948, 2016.